

# Fourth-Order Butterworth Active Bandpass Filter Design for Single-Sided Magnetic Particle Imaging Scanner

A. A. Sadiq<sup>1</sup>, N. B. Othman<sup>1</sup>, M. M. Abdul Jamil<sup>1</sup>, M. Youseffi<sup>2</sup>, M. Denyer<sup>2,3</sup>, W. N. Wan Zakaria<sup>4</sup>, and M. R. Md Tomari<sup>4</sup>

<sup>1</sup>Biomedical Modelling and Simulation Research Group, Faculty of Electrical and Electronics Engineering, Universiti Tun Hussein Onn Malaysia, Batu Pahat, Johor, Malaysia.

<sup>2</sup>School of Engineering, Design, and Technology, University of Bradford, Bradford, UK.

<sup>3</sup>School of Life Science, University of Bradford, Bradford, UK.

<sup>4</sup>Department of Mechatronics and Robotics Engineering, Faculty of Electrical and Electronics Engineering, Universiti Tun Hussein Onn Malaysia, Batu Pahat, Johor, Malaysia.  
engrsadiqgam@gmail.com

**Abstract**— This paper describes the design and simulation of a fourth-order Butterworth active bandpass filter designed for single-sided magnetic particle imaging (MPI) scanner. Bandpass filters (BPF) are used in MPI scanner set-up to attenuate the harmonic distortions generated by the power amplifier before passing the purely sinusoidal signal to the excitation (Drive) coils. The BPF is designed based on the excitation frequency of 22.8 kHz, having Butterworth response, and realized using Sallen-Key topology by cascading one second-order high-pass filter and one second-order lowpass filter, with values of the passive components calculated using the coefficient matching method. MATLAB and NI Multisim software are used to simulate the filter, and the results are compared. The magnitude response obtained using MATLAB have monotonic amplitude response in the pass and stopband, and maximally flat with small ripples in the passband than the NI Multisim implementation, while NI Multisim implementation has better roll-off than MATLAB implementation.

**Index Terms**—Bandpass filter; Harmonics; Magnetic particle imaging; MATLAB; NI Multisim.

## I. INTRODUCTION

Magnetic particle imaging (MPI) is an innovative imaging modality that applies oscillating magnetic fields to determine the distribution of magnetic nanoparticles. By using a pick-up (receive) coil, the change of the tracer magnetization can be sensed [1]. Nevertheless, the signal induced by the nanoparticles is overlaid by the direct feed through the intrusion of the time-varying excitation field, which couples into the receive coils. The oscillating magnetic field required to excite the magnetic nanoparticles used as the tracer is generated by Excitation (Drive) coil [2]. There is a need for the frequency of excitation to be clean on the coils to minimize harmonic distortions. Therefore, a high-quality Bandpass filter is required to attenuate all harmonics before the signal is applied to the excitation coils.

The typical signal flow of MPI scanner is as given in Figure 1. PA stands for the power amplifier, BPF is a bandpass filter,  $T_c$  stands for transmitting coil,  $R_c$  is receiving coil, BSF means bandstop filter, LNA is low noise amplifier while ADC is analog to digital converter.

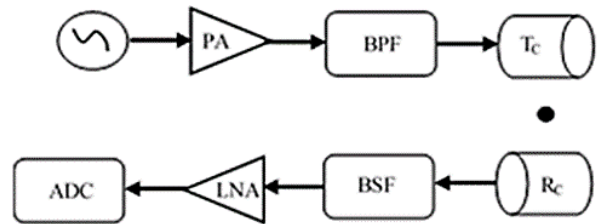


Figure 1: Signal chain of MPI scanner

The signal flow is divided into a transmitting section and a receiving section [3]. In the transmitting part, a sine wave signal is generated from a function generator at a fixed frequency. The excitation frequency is typically preferred to be around 25 kHz [2]. These frequencies normally are not detectable by the human ear, which makes the scanner operation not audible. There are also certain physiological limitations in the choice of the excitation frequency, as the scanner is designed for humans, so there is a limitation of exposure of human bodies to electromagnetic waves, one of those being energy deposition [4].

The AC sinusoidal signal generated is amplified by a power amplifier to achieve the desired currents. Since there are no ideal signal generators or power amplifiers, the amplified signal will contain not only the signal of the fixed excitation frequency but also different frequency components [5]. These frequency components (harmonics) have to be suppressed by a BPF before applying the signal to the drive coils [2, 5, and 6]. For this purpose, a third order Butterworth or Chebyshev II analog filter of high quality may be applied [2]. Going by this opinion a filter is needed in the scanner set up.

A filter is a circuit that is capable of passing a signal from input to output that allows frequency within the indicated band to pass and diminishing all others outside the band. They are four basic types of filters. They are lowpass, highpass, bandpass, and bandstop filter [7]. The simple filter is realized by different arrangements of resistors, capacitors, and occasionally inductors. It is known as a passive filter. Active filters make use of transistors or operational amplifier and RC circuit to provide wanted voltage gains or impedance features. Inductors are not ideal for active filter plan since it is slightest typical, massive, weighty, and costly and does not offer itself to IC-type mass production. Active filters are

usually employed in MPI scanner because they have excellent linearity, low power dissipation, large dynamic range and are easy to design and analyze [2].

Kwaha et al. (2011), developed and used a third-order infinite impulse response (IIR) lowpass Butterworth filter using the MATLAB direct method and bilinear transformation method. They reported that Butterworth filter design using bilinear transformation were more stable with a monotonically decreasing gain response, which is ascribed to its little roll-off associated with discrete components performance [8].

Similarly, Okubanjo and Oyetola (2012), designed and constructed a third-order unity gain Butterworth high pass active RC filter with a center frequency of 800 MHz. The filter was realized by cascading first and second order high pass filters together, employing the standard matching method to obtain the component values [9]. Additionally, Zehra (2014), designed and simulated a fourth-order active bandpass filter, comparing the multiple feedback and Sallen-key topologies. The filter designed has a Butterworth response with a pass band of 10-20 kHz, to be applied for radio frequency identification system (RFID). He carried out simulations using NI Multisim and MATLAB and reported that the bandpass filter designed using multiple feedback topology had a better performance as compared to Sallen-key topology [10].

For this research, a fourth-order Butterworth active bandpass filter is designed and implemented in National Instruments (NI) Multisim and compared with MATLAB direct method simulation. It is expected at the output of the filter to have a signal with 22.8 kHz center frequency and a unity gain, with the unwanted harmonics, attenuated.

## II. RESEARCH METHOD

### A. Bandpass Filter (BPF) Design

A band-pass filter (BPF) permits all signals lying inside a band in the middle of low and high critical frequency limits and discards all other frequencies beyond this band. Bandpass filter comprises a high-pass filter (HPF) and a low-pass filter (LPF). It is realized by cascading the circuits for HPF and LPF [11]. Therefore, BPF is divided into two sections that are analyzed separately to determine the values of the RC components. The magnitude response of a BPF is shown in Figure 2.

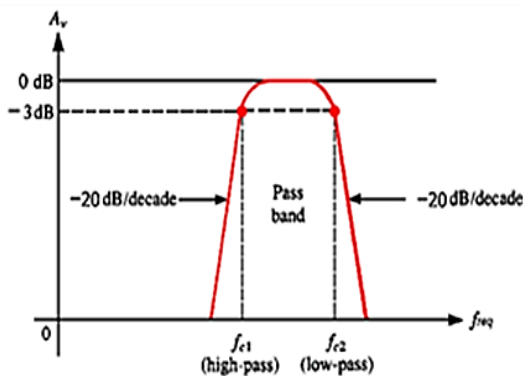


Figure 2: Band Pass Filter Magnitude Response

The conventional two-pole active filter is displayed in Figure 3 with  $Y_1$  through  $Y_4$  are admittances and with an ideal voltage follower. Figure 3 is used to design either a highpass

or lowpass filter, depending on the type admittances. BPF is a combination of highpass, and lowpass filters cascaded together.

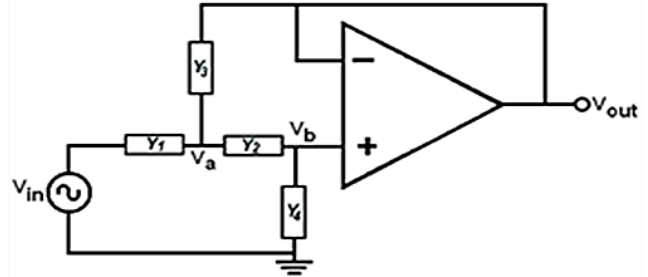


Figure 3: A unity gain conventional 2-pole active filter

A KCL Equation at node  $V_a$  shall be:

$$(V_{in} - V_a)Y_1 = (V_a - V_b)Y_2 + (V_a - V_{out})Y_3 \quad (1)$$

A KCL Equation at node  $V_b$  produces

$$(V_a - V_b)Y_2 = V_b Y_4 \quad (2)$$

For ideal op-amps,  $V_b$  is also equal to  $V_{out}$ . Therefore,

$$V_a = \left[ \frac{Y_2 + Y_4}{Y_2} \right] V_b = \left[ \frac{Y_2 + Y_4}{Y_2} \right] V_{out} \quad (3)$$

Thus, substitute Equation three into Equation (1) and multiply it by the term  $Y_2$ , it yields the transfer function  $T(s)$  for the filter, which is

$$T(s) = \frac{V_{out}(s)}{V_{in}(s)} = \left[ \frac{Y_1 Y_2}{Y_1 Y_2 + Y_4 (Y_1 + Y_2 + Y_3)} \right] \quad (4)$$

Equation (4) is the general transfer function equation for a 2-pole active filter. This Equation can be used to determine the transfer function of a 2-pole high pass or 2-pole low pass filter depending on the admittance [12]. Therefore, Equation four is utilized in the low-pass and high-pass filters design to determine the values of the RC components required to realize a BPF.

#### 1) Low-pass Filter Design

Substituting  $Y_1 = 1/R_1$ ,  $Y_2 = 1/R_2$ ,  $Y_3 = sC_1$  and  $Y_4 = sC_2$  into Equation (4) gives:

$$T(s) = \frac{V_{out}(s)}{V_{in}(s)} = \left[ \frac{1/R_1 R_2 C_1 C_2}{s^2 + \frac{(R_1 + R_2) s C_2}{R_1 R_2 C_1 C_2} + 1/R_1 R_2 C_1 C_2} \right] \quad (5)$$

The transfer function can also be organized as the standard second-order low-pass network Equation, which is:

$$T(s) = \frac{\omega_c^2}{s^2 + 2\epsilon\omega_c s + \omega_c^2} \quad (6)$$

Therefore, the center frequency,

$$f_c = \frac{1}{2\pi\sqrt{R_1R_2C_1C_2}}$$

If  $R_1 = R_2 = R$ ,  $\tau_1 = RC_1$  and  $\tau_2 = RC_2$  then;

$$f_c = \frac{1}{2\pi\sqrt{\tau_1\tau_2}} = \frac{1}{2\pi R\sqrt{C_1C_2}} \quad (7)$$

### 2) High-pass Filter Design

For a high pass filter design, the following are substituted into Equation (4) as follows:

$Y_1 = sC_1$ ,  $Y_2 = sC_2$ ,  $Y_3 = 1/R_1$  and  $Y_4 = 1/R_2$  which yields:

$$T(s) = \frac{V_{out}(s)}{V_{in}(s)} = \frac{SC_1 \cdot SC_2}{SC_1 \cdot SC_2 + 1/R_2 (SC_1 + SC_2 + 1/R_1)} \quad (8)$$

Comparing Equation (8) and the standard transfer function,

$$T(s) = \frac{S^2}{S^2 + 2\varepsilon\omega_c S + \omega_c^2} \quad (9)$$

Therefore, the center frequency is:

$$f_c = \frac{1}{2\pi\sqrt{R_1R_2C_1C_2}}$$

If  $C_1 = C_2 = C$  and  $\tau_1 = R_1C$  and  $\tau_2 = R_2C$  then;

$$f_c = \frac{1}{2\pi\sqrt{\tau_1\tau_2}} = \frac{1}{2\pi C\sqrt{R_1R_2}} \quad (10)$$

### B. Band-Pass Filter Design Considerations

The first factor in BPF design is the center frequency  $f_0$ , which is given as:

$$f_0 = \sqrt{f_1f_2} \quad (11)$$

where  $f_1$  is the lower frequency band to be passed (edge of the passband) and  $f_2$  is the upper frequency band to be passed (closing edge of the passband). The second consideration in BPF design is the bandwidth (BW) of the filter given as:

$$BW = f_2 - f_1 \quad (12)$$

Quality factor,

$$Q = \frac{f_0}{BW} \quad (13)$$

If the quality factor Q is less than 10, a wide BPF with the flat response over a range of frequencies will be realized. Bandwidth is more in this case. Whereas if Q is greater than 10, then a narrow BPF with a sharp bell type response will be achieved. Bandwidth is less in this case [13].

For the single-sided MPI scanner to be constructed, a 25 kHz excitation frequency is preferred [2]. Meanwhile,  $f_1$  and  $f_2$  were arbitrarily selected below and above the excitation frequency we have in mind, so as to fully capture the excitation frequency within the pass band. Therefore  $f_1$  was chose as 20 kHz while  $f_2$  as 26 kHz.

$$f_0 = \sqrt{f_1f_2} = 22.8 \text{ kHz}, BW = 6 \text{ kHz} \text{ and } Q = 3.8$$

With  $Q = 3.8$ , we have a wide BPF with a bandwidth of 6 kHz.

In order to maintain the filter stability, a gain of the active filter must not be greater than 3, which is best expressed as:

$$A = 3 - (2 \times \zeta) \quad (14)$$

where A stands for the overall gain of the op-amp and  $\zeta$  is the damping factor, given as:

$$\zeta = \frac{3 - A}{2} = \frac{1}{2Q}$$

Therefore,  $A = 3 - 1/Q$ . With  $Q = 3.8$ , the gain  $A = 2.74 \approx 3$ . Hence, a gain of  $A = 3$  is assumed.

#### a) High-pass Filter Section

The first part of the BPF is the HPF section. Here, the center frequency  $f_c$  is the lower frequency band to be passed,  $f_1$  (20 kHz). For simplicity, capacitors  $C_1 = C_2 = C$  and is picked to be 470 pF (standard), while the resistors values are calculated as follows:

Using the passband gain of 3,

$$A = 1 + \frac{R_2}{R_1} = 3 \quad (15)$$

From Equation (15), it implies that  $R_2 = 2R_1$ . Substituting for  $R_2$  into Equation (10) yields:

$$R_1 = \frac{1}{2\pi\sqrt{2}f_2C} \quad (16)$$

Substituting the values for  $f_c$ ,  $R_1$  and  $R_2$  into Equation (13) gives:

$$R_1 = 11,972.29 \Omega \text{ or } 11.97229 \text{ k}\Omega$$

Standard resistor value of 12 k $\Omega$  is chosen and since  $R_2 = 2R_1 = 24 \text{ k}\Omega$

#### b) Low-pass Filter Section

The center frequency  $f_c$  for the Low-pass section of the BPF is the upper frequency band to be passed,  $f_2$  (26 kHz). Here, the assumption made using the passband gain of 3 is that:  $R_1 = R_2 = R$  and;

$$A = 1 + \frac{C_1}{C_2} = 3 \quad (17)$$

which implies that  $C_1 = 2C_2$ . Here,  $C_1$  was chosen as 470 pF. Consequently,  $C_2 = 940 \text{ pF}$ . The resistor value is calculated from Equation 7, which gives:

$$R = \frac{1}{2\pi f\sqrt{C_1C_2}} = 9,209.46 \Omega \text{ or } 9.21 \text{ k}\Omega$$

Therefore, a standard resistor value of 10 k $\Omega$  was chosen.  $R_1 = R_2 = R = 10 \text{ k}\Omega$

Table 1 below gives the summary of the RC components for the BPF, calculated for the HPF and LPF sections.

Table 1  
Overview of BPF RC Components

Section	$f_c$ (kHz)	$C_1$ (pF)	$C_2$ (pF)	$R_1$ (k $\Omega$ )	$R_2$ (k $\Omega$ )
HPF	20	470	470	12	24
LPF	26	470	940	10	10

Figure 4 shows a fourth-order Butterworth active filter schematic which is to be implemented in NI Multisim.

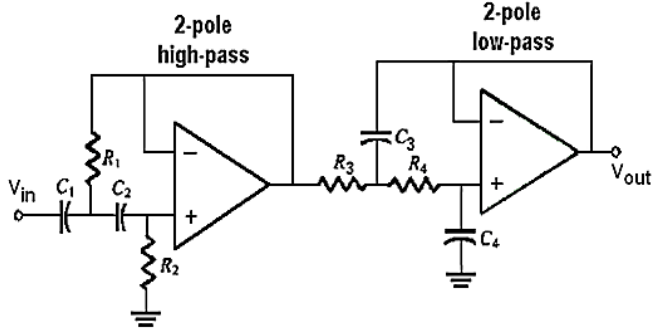


Figure 4: Fourth-order Butterworth active BPF schematic diagram

C. BPF Design Implementation

The behavior of BPF to be designed with the parameters presented in Table 1 is simulated in NI Multisim software and MATLAB. Multisim is a comprehensive development platform for electronic circuit’s schematics, designs simulation, and prototyping. MATLAB, on the other hand, provides high-performance numerical calculation, data analysis, visualization capabilities and application development tools. The results obtained from the two simulations are presented and compared.

a) NI Multisim Implementation

The BPF schematic diagram given in Figure 4 is implemented in NI Multisim with the values of the RC components in Table 1. Where R1, R2 equal to R3, R4 for the LPF section, likewise C1, C2 equals C3 and C4 for LPF section respectively. NI Multisim implemented circuit was as shown in Figure 5.

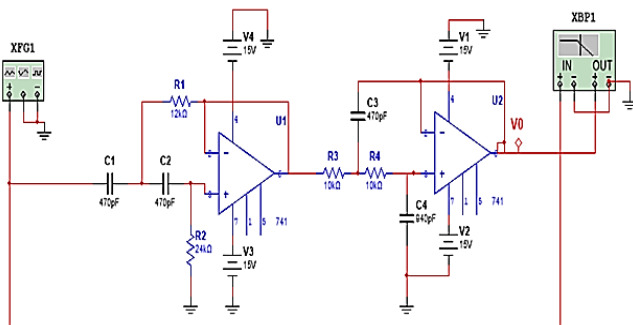


Figure 5: NI Multisim circuit implemented for Fourth-order Butterworth active BPF.

b) MATLAB Implementation

Unlike the NI Multisim application, MATLAB direct method uses the frequency specifications only in designing the filter [14]. These frequency specifications are written in code and evaluated in MATLAB after a prompt command, called the *fdesign.Bandpass* (Bandpass filter design method). The frequency specifications of the magnitude response of a BPF is given in Figure 6 below.

Astop1 is the Attenuation in the first stopband; Fstop1 is Edge of the stopband while Fpass1 and Fpass2 are the Edges of the Opening and Closing of the passband respectively. Other parameters are Fstop2, which is the Edge of the second stopband; Astop2 is Attenuation in the second stopband and APass is the amount of ripple allowed in the passband. Fs is the sampling frequency.

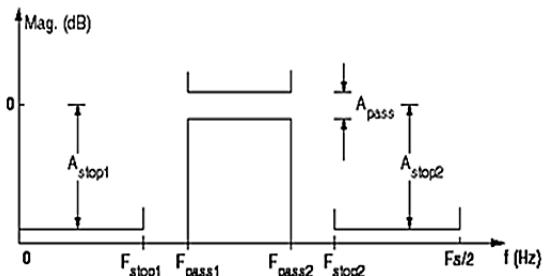


Figure 6: BPF magnitude response frequency specifications using MATLAB

The values of these parameters used are given in Table 2. For creating the filter specification object, a code is evaluated at the MATLAB prompt [15]. With the excitation frequency of 25 kHz for the MNPs sample, a range of 20-26 kHz is logically selected as the actual portion of the affected spectrum, so that the center frequency will be captured within this range. This selection gives a center frequency of 22.8 kHz (Equation 15). 20 kHz is the first passband frequency (Fpass1) while 26 kHz is the closing passband frequency (Fpass2) [18].

In practice, no BPF is ideal. Therefore, the attenuation in the first and second stopband have to be wide enough, to make the roll-off as narrow as possible. 60 dB is the default value adopted for a wider transition region. For linearity, 15 kHz and 30 kHz were chosen as the edge of the first and second stopband respectively (Fstop1 and Fstop2). The sampling frequency is twice the frequency of the edge (45 kHz), which is 90 kHz [16]. The amount of ripple to be seen in the passband is up to the filter designer to choose. A ripple of 1% is allowed in this design (0.1 dB) because the design is based on a mathematical function which is used to produce maximally flat passband with no considerations for phase linearity or group delay discrepancies [17].

Table 2  
MATLAB BPF Specifications

AStop	FStop	FPass	FPass	FStop	AStop	APas	F <sub>s</sub>
(dB)	(kHz)	(kHz)	(kHz)	(kHz)	(dB)	(dB)	z
60	15	20	26	30	60	0.1	90

III. RESULTS AND ANALYSIS

Simulations were carried out using MATLAB and NI Multisim software, and the results are presented in Figure 7 and Figure8 respectively. The Fourth-order Butterworth active BPF simulated in MATLAB exhibit very flat amplitude in its passband (maximally flat), as shown in Figure 7. The response of the filter is smooth with a roll-off rate of -80dB/pole and 80dB/pole. The pass and stop frequency have an amplitude response at -3dB while the center frequency has zero gain as this is in line with the characteristics of BPF [18]. The center frequency has zero phase while the stop frequency (20 kHz) and pass frequency (26 kHz) have phases of 2 and -2 radians respectively. Nevertheless, the phase shift of the signals going through the filter differs nonlinearly with the frequencies.

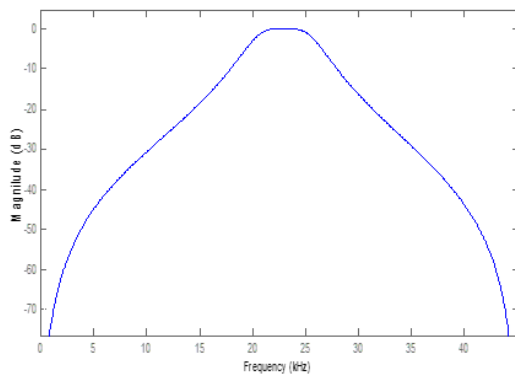


Figure 7: BPF magnitude response using MATLAB

The result of the NI Multisim simulation and experiment for the Fourth-order Butterworth active BPF is shown in Figure 8. The circuit implemented for the filter is given in Figure 5. The magnitude response exhibits a flat amplitude in the passband but not as maximally flat as that of MATLAB simulation. The response of the filter is smooth with steeper roll-off than MATLAB simulation [16]. The pass and stop frequency have the same amplitude response as that of MATLAB simulation, at -3dB point. The phase response is nonlinear, with the center frequency having zero phase and the pass and stop frequencies having -5 and 5 radians respectively.

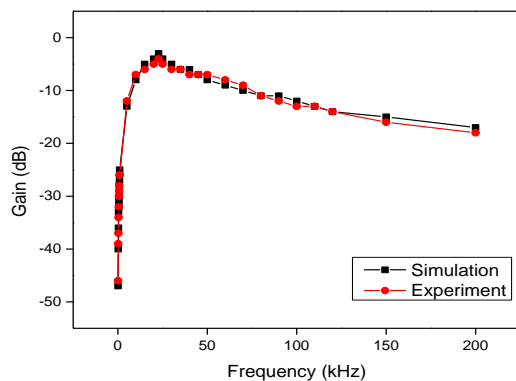


Figure 8: BPF magnitude response for NI Multisim simulation and experiment

In comparison, the BPF simulated in MATLAB have monotonic amplitude response in the pass and stopband, have maximally flat and small ripples in the passband than the NI Multisim implementation. Regarding a better roll-off towards zero in the stopband, NI Multisim implementation is better. The better roll-off is due to the fast roll-off noticed around the center frequency as shown in Figure 8. MATLAB simulation also yields a more linear phase response in the passband as compared to the slightly nonlinear phase response of the NI Multisim simulation. The two simulation works are significant for the MPI scanner realization.

#### IV. CONCLUSION

The design and implementation of a fourth-order Butterworth active bandpass filter are presented in this paper. Both simulation results reveal that the magnitude and phase

response of the realized BPF is close to the ideal characteristics of a fourth-order active BPF having Butterworth characteristics. The little difference is due to the approximations in calculating component values (resistors and capacitors) in NI Multisim implementation. Even though there is no boundary to the order of the filter that can be formed, the fourth-order design is suitable for the MPI scanner design because of the higher the filter order, the better the performance of the filter. The rate of roll-off and the width of the filter transition band also depends on the filter order.

#### ACKNOWLEDGMENT

This research was conducted with financial support by Research Acculturation Grant Scheme (RAGS) Vot number R067 and Postgraduate Research Grant (GPPS) Vot number U589, Universiti Tun Hussein Onn Malaysia (UTHM).

#### REFERENCES

- [1] Gleich and J. Weizenecker, "Tomographic imaging using the nonlinear response of magnetic particles," *Nature*, vol. 435, pp. 1214-1217, 2005.
- [2] T. Buzug, G. Bringout, M. Erbe, K. Gräfe, M. Graeser, M. Grüttner and J. Haegle, "Magnetic particle imaging: Introduction to imaging and hardware realization," *Zeitschrift für Medizinische Physik*, vol. 22, pp. 323-334, 2012.
- [3] S. Biederer, T. Knopp, T. Sattel, K. Lüdtke-Buzug, B. Gleich, J. Weizenecker and T. Buzug, "Magnetization response spectroscopy of superparamagnetic nanoparticles for magnetic particle imaging," *Journal of Physics D: Applied Physics*, vol. 42, pp. 205007, 2009.
- [4] T. Knopp, and T. Buzug, "Magnetic particle imaging: an introduction to imaging principles and scanner instrumentation," Springer Science & Business Media, 2012.
- [5] H. Rogge, and R. Schneider, "Magnetic Particle Imaging (Doctoral dissertation, Diploma thesis)," 2011.
- [6] A. Sadiq, N. Othman, and M. Mahadi, "Magnetic particle imaging system for cancer diagnosis: an overview," *ARPN Journal of Engineering and Applied Sciences*, vol. 10, pp. 8556-8561, 2015.
- [7] R. Levy, R. Snyder, and G. Matthaei, "The design of microwave filters. Microwave Theory and Techniques," *IEEE Transactions on Microwave Theory and techniques*, vol. 50, pp. 783-793, 2002.
- [8] B. Kwaha, O. Inyang, and P. Amalu, "The circular microstrip patch antenna—design and implementation," *International Journal of Research and Reviews in Applied Sciences*, vol. 8, pp. 86-95, 2011.
- [9] A. Okubanjo and K. Oyetola, "Design, construction, and simulation of third order Butterworth high-pass filter using MATLAB," *Research gate*. Retrieved 13 June 2016, 2012.
- [10] A. Zehra, "Design and simulation of 4th order active bandpass filter using multiple feedback and Sallen key topologies," *Journal of Babylon University*, vol. 2, pp. 463-473, 2014.
- [11] T. Deliyannis, Y. Sun and J. Fidler, "Continuous-time active filter design," CRC Press, 1998.
- [12] J. Kuo and E. Shih, "Wideband bandpass filter design with three-line microstrip structures," In *Microwaves, Antennas, and Propagation, IEE Proceedings*, vol. 149, pp. 243-247, 2002.
- [13] V. Bhagavatula, "Power and area optimization techniques for ultra-wideband millimeter-wave CMOS transceivers," *Doctoral dissertation*, 2014.
- [14] M. Lutovac, D. Tošić, and B. Evans, "Filter design for signal processing using MATLAB and Mathematica," Miroslav Lutovac, 2001.
- [15] A. Casson, D. Yates, S. Patel and E. Rodriguez-Villegas, "An analog bandpass filter realization of the continuous wavelet transform," In *2007 29th Annual International Conference of the IEEE Engineering in Medicine and Biology Society*, 2007 Aug 22, pp. 1850-1854, 2007.
- [16] S. Winder, "Analog and digital filter design," Newnes, 2002.
- [17] A. Biswal and V. Profile, "Butterworth filter and Chebyshev filter – A comparison," 2012.
- [18] H. Ishida and K. Araki, "Design and analysis of UWB band pass filter with ring filter," In *Microwave Symposium Digest, 2004 IEEE MTT-S International*, vol. 3, pp. 1307-1310, 2004.